

# Substitution at the F-Ring *N*-Imide of the Indolocarbazole Antitumor Drug NB-506 Increases the Cytotoxicity, DNA Binding, and Topoisomerase I Inhibition Activities

Christian Bailly,<sup>\*,‡</sup> Xiaogang Qu,<sup>§</sup> Jonathan B. Chaires,<sup>§</sup> Pierre Colson,<sup>‡</sup> Claude Houssier,<sup>‡</sup> Mitsuru Ohkubo,<sup>||</sup> Susumu Nishimura,<sup>||</sup> and Tomoko Yoshinari<sup>||</sup>

Laboratoire de Pharmacologie Antitumorale du Centre Oscar Lambret and INSERM U-524, IRCL, Lille 59045, France, Department of Biochemistry, University of Mississippi Medical Center, Jackson, Mississippi 39216, Laboratoire de Chimie Macromoléculaire et Chimie Physique, Université de Liège, Liège 4000, Belgium, and Banyu Tsukuba Research Institute, Okubo, Tsukuba, Japan

Received February 18, 1999

The antitumor drug NB-506, which is currently undergoing phase I/II clinical trials, contains a DNA-intercalating indolocarbazole chromophore substituted with a glucose residue. In addition to interacting with DNA, the drug stabilizes the topoisomerase I–DNA covalent complex. To reinforce the DNA binding and anti-topoisomerase I activities of NB-506, an analogue containing a new substituent on the naphthalimide ring F was synthesized. The *N*-formylamino group of NB-506 has been replaced with a more hydrophilic group, *N*-bis-(hydroxymethyl)methylamino. In this study we show that the incorporation of a longer substituent on the N6 position effectively reinforces both the interaction with DNA and the capacity of the drug to maintain the integrity of the topoisomerase I–DNA covalent complexes. The strength and the mode of binding of the drugs to DNA were studied by complementary biophysical techniques including absorption, fluorescence, and circular and linear dichroism. Various biochemical procedures were applied to investigate the effects on human topoisomerase I using plasmid DNA as well as restriction fragments. The drug binding sites and the positions of the topoisomerase I-mediated cleavage sites were mapped with nucleotide resolution using footprinting and sequencing techniques. Cytotoxicity measurements performed with various human cancer cell lines (HCT-116, DLD-1, MKN-45) indicate that the newly designed drug is 3 to 4 times more toxic to colon and gastric cancer cells than NB-506. Therefore, the results suggest that the antitumor activity of indolocarbazole-based drugs can be enhanced by incorporating DNA and/or topoisomerase I reactive groups. They also support the hypothesis that the substituent on the imide nitrogen on the F ring of NB-506 has direct interaction with the molecular target. The study helps to define the structure–activity relationships in the indolocarbazole series of antitumor agents targeting topoisomerase I.

## Introduction

In 1991, the antibiotic BE13793C (Chart 1) was isolated from culture supernatants of a *Streptoverticillium* species.<sup>1</sup> This indolocarbazole derivative has shown remarkable activity in Ehrlich ascites tumor cells, but its very low aqueous solubility has hampered further evaluation. To increase the solubility in water, a glycosyl derivative of BE13793C was prepared by hemi-synthesis.<sup>2</sup> The resulting compound, named ED-110, was shown to be extremely toxic against a panel of tumor cell lines, including cells resistant to vincristine and adriamycin.<sup>3</sup> ED-110 is also very potent at inhibiting the growth of murine and human solid tumors in mice.<sup>4</sup> Then the substitution of ED-110 with a *N*-formylamino group led to the most active compound in the series, NB-506 (Chart 1), which is active in vivo and is currently undergoing clinical trials.<sup>5–8</sup>

NB-506 and related indolocarbazole compounds are very potent inhibitors of topoisomerase I both in vitro and in cellular systems.<sup>9–11</sup> Their effects on the DNA relaxation and cleavage activities of topoisomerase I are very similar to those observed with the camptothecins. In addition, NB-506 directly interacts with DNA and inhibits DNA and RNA polymerases.<sup>12</sup> In terms of DNA binding, NB-506 and analogues are best compared with the anthracyclines (e.g., adriamycin, daunomycin), which also possess a planar chromophore substituted with a glycosyl side chain, rather than with the camptothecins which have very weak, if any, interaction with DNA in the absence of topoisomerase I. However, it is important to mention that nearly all compounds in the NB-506 series are uncharged whereas the vast majority of DNA binding ligands are positively charged.

NB-506 specifically stimulates DNA cleavage by topoisomerase I without any effect on topoisomerase II.<sup>3,9</sup> This mechanism of action is not restricted to the indolocarbazoles. Numerous topoisomerase I poisons including the camptothecins and DNA minor groove binders, such as Hoechst 33258, and DNA intercalators, such as benzophenanthridine alkaloids, have been

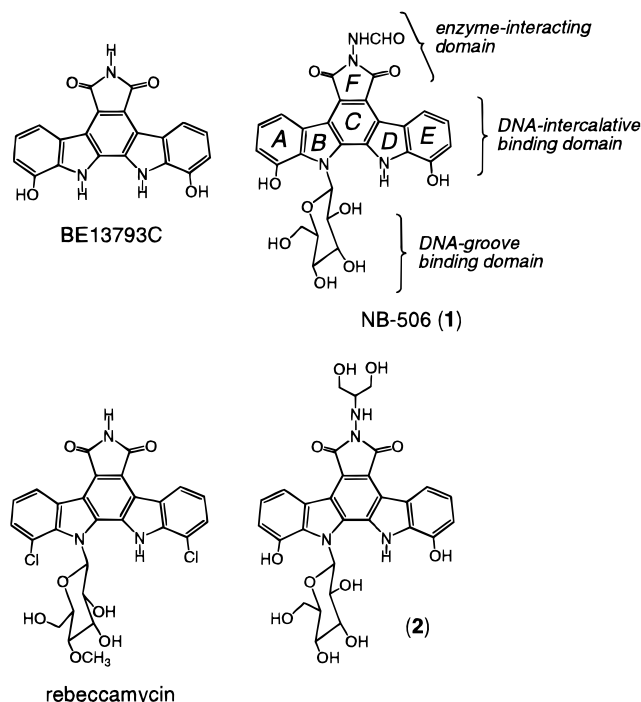
\* To whom requests for reprints and correspondence should be addressed. Fax: (+33) 320 16 92 29. E-mail: bailly@lille.inserm.fr.

‡ INSERM U-524.

§ University of Mississippi.

‡ Université de Liège.

|| Banyu Research Institute.

Chart 1<sup>a</sup>

<sup>a</sup> The three functional domains of NB-506 (**1**) are indicated. The planar indolocarbazole chromophore can intercalate into DNA while the carbohydrate residue contacts externally the DNA in the (minor) groove. Previous studies suggested that the bis-imide F ring and its substituent play a direct role in the interaction with topoisomerase I.<sup>22</sup>

discovered and developed.<sup>13–15</sup> Over the last three years, over 100 analogues of the antibiotic rebeccamycin (Chart 1), which is structurally related to NB-506, have been synthesized.<sup>16–21</sup> On the basis of structure–activity relationships studies, the structure of rebeccamycin-type drugs can be divided into three functional domains.<sup>22</sup> The planar indolocarbazole chromophore intercalates between two consecutive base pairs, disposing the appended sugar residue into the groove of the double helix, most likely the minor groove.<sup>23</sup> The substituent on the imide nitrogen on the F ring is supposed to protrude toward the opposite groove where it can interact with topoisomerase I. According to this molecular arrangement, it seems possible to reinforce the interaction of the drug with DNA and/or topoisomerase I by incorporating a longer substituent on the N6 position. This hypothesis has been experimentally tested by comparing the DNA binding and topoisomerase I poisoning activities of compounds **1** and **2** shown in Chart 1. The *N*-formylamino group of NB-506 (**1**) has been replaced with a more hydrophilic group, *N*-bis-(hydroxymethyl)methylamino.

## Results

**Interaction with DNA. 1. Affinity.** Different methods were employed to compare the DNA binding properties of **1** and **2**. First we investigated the effects of the drugs on the thermal denaturation of calf thymus DNA (Figure 1). The two compounds weakly stabilize duplex DNA against thermal denaturation. The stabilizing effect ( $\Delta T_m$ ) is, however, slightly more pronounced with **2** than with **1**. Next we titrated solutions of the drug at a fixed concentration with increasing concentrations of

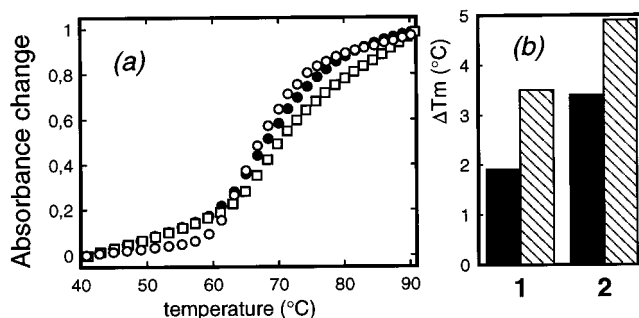


**Figure 1.** (a) Thermal denaturation curves for calf thymus DNA (○) in the absence and presence of (●) **1** and (□) **2** at a drug/DNA ratio of 0.25. (b) Comparison of the  $\Delta T_m$  values ( $T_m$  complex –  $T_m$  DNA) measured for **1** and **2** at a drug/DNA ratio of 0.5 (solid bars) and 1 (hatched bars). The  $T_m$  values were obtained from first-derivative plots.

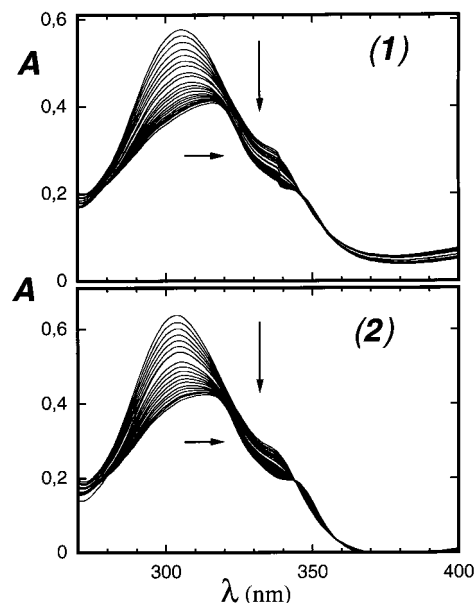


**Figure 2.** Absorption titrations for the interaction of **1** and **2** with calf thymus DNA. The figure contains the absorption spectrum of the free drug, intermediate spectra, and final spectra of the drug–DNA complexes, in which the ligands have been sequestered completely by the DNA. To 3 mL of drug solution (20  $\mu$ M in BPE buffer) were added aliquots of a concentrated CT-DNA solution. Spectra are referenced against DNA solutions of exactly the same DNA concentration and were adjusted to a common baseline at 450 nm. The phosphate-DNA/drug ratio increased from 0 to 7 (top to bottom curves, at 305 nm).

DNA. The absorption spectra of the free and DNA-bound drugs were recorded between 270 and 400 nm (Figure 2). In both cases, the main absorption band centered at 305 nm is shifted to 315 nm. Binding of the drugs to DNA induces well-defined bathochromic and hypochromic effects. At high P/D (DNA phosphate over drug) values, a red shift of about 11 nm and 30% hypochromicity are observed. During titration with DNA, an isosbestic point at 345 nm is present, pointing to the existence of a single binding mode (Figure 2). The spectral shifts are slightly more pronounced with **2** than with **1**. Together with the  $\Delta T_m$  data, the UV–vis spectra suggest that the introduction of the longer side chain at the N6 position enhances the interaction of **1** with DNA, as it was expected. Fluorescence measurements fully confirmed this belief.

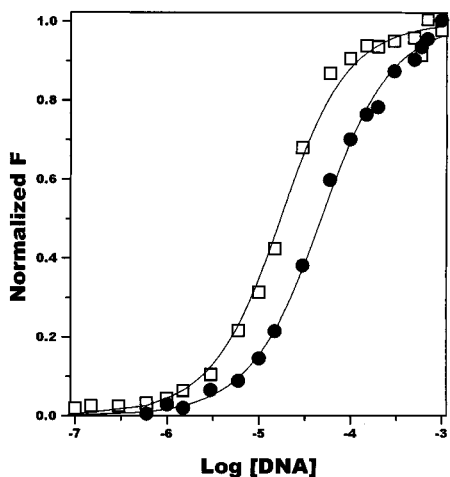


**Figure 3.** Fluorescence titrations for the interaction of **1** and **2** with calf thymus DNA. The normalized fluorescence response,  $\theta = (F - F_0)/(F_b - F_0)$ , is shown as a function of total DNA concentration. The concentration of ligand was kept constant at 5  $\mu\text{M}$  while the DNA concentration was varied between 1 mM and 0.1  $\mu\text{M}$  bp. Curve fitting and determination of binding constants (Table 1) were carried out by using nonlinear least-squares analysis, as described in the text. The solid lines show the best fit curves to the binding model described in the text.

We exploited the intrinsic fluorescence of the indolocarbazole chromophore to evaluate the strength of the interaction of the drugs with calf thymus DNA. The fluorescence emission at 560 nm is weak when the drug is free in solution but it is considerably enhanced when the drug is bound to DNA. This property is very useful for accurate determination of the DNA binding affinities. Nonlinear least-squares analysis of the fluorescence titration curves shown in Figure 3 yielded binding constants of  $2.6 \times 10^4 (\text{M bp})^{-1}$  and  $8.2 \times 10^4 (\text{M bp})^{-1}$  for **1** and **2**, respectively, in low salt BPE buffer at neutral pH. There is no doubt that the replacement of the NHCHO group of **1** with a NHCH(CH<sub>2</sub>OH)<sub>2</sub> substituent significantly enhances the binding to DNA. The affinity constant of **2** is 3-fold higher than that of **1**.

Both drugs are uncharged, in contrast to the vast majority of DNA intercalating agents known so far. The binding constants measured in the presence of increasing NaCl concentrations show little variation. The SK  $[(\delta \log K)/(\delta \log [\text{Na}^+])]$  value measured for **1** is  $-0.23$ , i.e., nearly identical to the theoretical value of  $-0.24$  predicted for the binding of an uncharged intercalator to DNA.<sup>24</sup> The value measured for **2** is also well below  $-1$ . A theoretical value of  $-0.88$  to  $-1.24$  is predicted for a ligand bearing one positively charged group.<sup>24,25</sup> These experiments suggest that the two NH groups of **2** (the free NH indole and the NH on the newly introduced substituent) are not protonated upon interaction of the drug with DNA at neutral pH, as expected.

The free energy of drug binding to DNA was estimated.  $\Delta G_{\text{obs}}$  was calculated from the binding constants using the standard Gibbs relation  $\Delta G_{\text{obs}} = -RT \ln K$ . The observed binding free energy can then be partitioned into its nonpolyelectrolyte contribution ( $\Delta G_t$ ) and its polyelectrolyte contribution ( $\Delta G_{\text{pe}}$ ).<sup>26</sup> The  $\Delta G_{\text{pe}}$  values reported in Table 1 indicate that both **1** and **2** bind to DNA with a favorable polyelectrolyte contribution. The values of  $\Delta G_t$  are the same for the two drugs and are the major contributors to  $\Delta G_{\text{obs}}$ . These values indicated

**Table 1.** Binding Constants and Energetics of the Drugs Binding to DNA

	<b>1</b>	<b>2</b>
$K/10^4 (\text{M}^{-1})$	2.64	8.19
$-\Delta G_{\text{obs}} (\text{kcal/mol})$	5.91	6.56
$-(\delta \log K)/(\delta \log [\text{Na}^+])$	0.23	0.41
$-\Delta G_{\text{pe}} (\text{kcal/mol})$	0.56	0.98
$-\Delta G_t (\text{kcal/mol})$	5.35	5.58

<sup>a</sup> Binding constant ( $K$ ) and standard free energy changes ( $\Delta G_{\text{obs}}$ ) refer to solution conditions of 6 mM Na<sub>2</sub>HPO<sub>4</sub>, 2 mM NaH<sub>2</sub>PO<sub>4</sub>, and 1 mM Na<sub>2</sub>EDTA, pH 7.0, at 20 °C. The polyelectrolyte contribution to the standard free energy change was calculated from the relationship  $\Delta G_{\text{pe}} = (\text{SK})RT \ln [\text{NaCl}]$ , where SK =  $(\delta \log K)/(\delta \log [\text{Na}^+])$ . The thermodynamic free energy change was calculated by difference,  $\Delta G_t = \Delta G_{\text{obs}} - \Delta G_{\text{pe}}$ .

that the binding of the two drugs to DNA is primarily stabilized by molecular interactions other than the polyelectrolyte effect, such as van der Waals interactions and possibly hydrogen-bonding interactions.

**2. Geometry of Intercalated Drug–DNA Complexes.** The mode of binding to DNA was investigated by circular dichroism (CD) and electric linear dichroism (ELD). Addition of calf thymus DNA induces significant changes in the CD spectra of the two drugs (Figure 4a,b). In both cases, the band at 340 nm decreases as the DNA concentration is raised; meanwhile the CD in the 310–330 nm region increases significantly. In the presence of DNA, the variation in CD intensity at 340 nm is more or less equivalent for the two drugs (Figure 4c). The binding appears geometrically homogeneous.

Figure 5 shows a typical set of experimental data for the dependence of the reduced dichroism  $\Delta A/A$  on (a) the wavelength, (b) the DNA/drug ratio, and (c) the electric field strength. The binding mode can be determined only on the basis of the highest ELD values, obtained when the drug molecules are fully bound to DNA, i.e., for P/D ratios larger than 10. At lower P/D ratio, the measured ELD values fall significantly due to the appearance of unbound molecules in the solution. The ELD spectra of **1**– and **2**–DNA complexes indicate that the reduced dichroism is always negative in sign, even in the 300–360 nm region where the indolocarbazole chromophore absorbs the light. This situation differs from that reported previously with minor groove binders such as netropsin and distamycin which exhibited positive reduced dichroism signals around 320 nm.<sup>27</sup> The intensity of the ELD signal is a function of the degree of alignment of the DNA molecules in the electric field. With both drugs, there is a clear parallelism between the electric field dependence of the reduced dichroism measured at 260 nm for the DNA bases and at 330 nm for the drugs (Figure 5c). This indicates that the planar indolocarbazole ring is tilted close to the plane of the DNA bases, consistent with an intercalative mode of binding.

Further ELD studies were undertaken to compare the binding of the drugs to various synthetic polynucleotides. Measurements were carried out at a fixed P/D ratio of 20 and under the same buffer and temperature conditions for the two compounds. The results in Figure 6 confirm that the geometry of intercalated drug molecules is always identical with **1** and **2** whatever the sequence of the DNA. In both cases, the dichroism ratios are close to +1, i.e., the expected value for a drug parallel to the DNA base pair plane. We must conclude

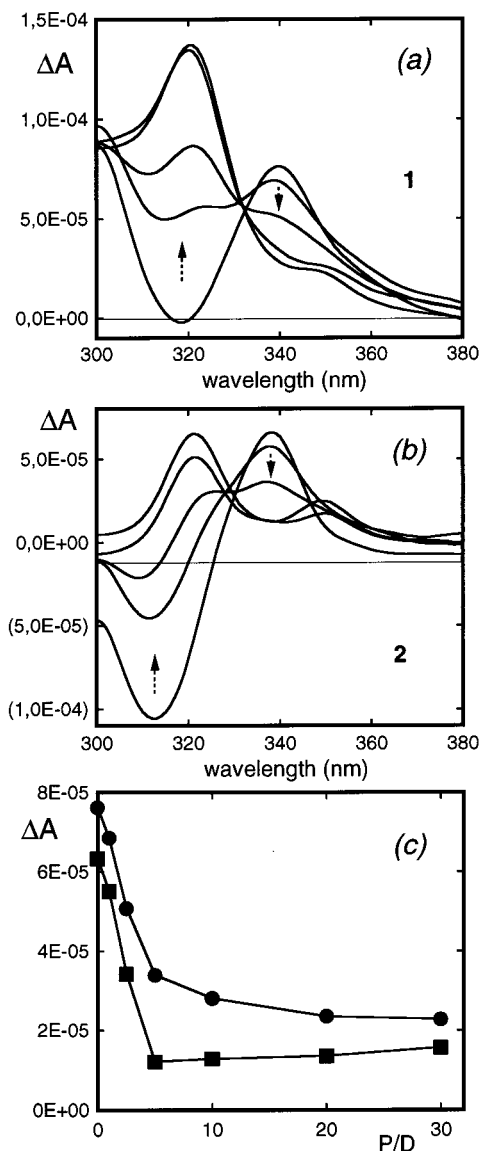


**Figure 4.** Circular dichroism. Titration of (a) **1** and (b) **2** with calf thymus DNA. Panel c shows the variation of the circular dichroism amplitude  $\Delta A$  measured at 340 nm as a function of the DNA-phosphate/drug ratio (P/D) for (●) **1** and (■) **2**. In panels a and b, the DNA-phosphate/drug ratio (P/D) increased as follows (bottom to top curves at 310 nm): 0, 1, 2.5, 5, 10.

that both **1** and **2** can intercalate into DNA whatever the sequence. The variation observed with the different polynucleotides may reflect various extents of drug-induced stiffening of the double helix.

**3. Sequence Selectivity.** The 117-mer *EcoRI-PvuII* fragment of the pBS plasmid was used in DNAase I footprinting experiments. The DNA fragment, radiolabeled at the 3'-end at the *EcoRI* site, was incubated with the test drugs at various concentrations, and then the drug-DNA complexes were subjected to limited endonuclease cleavage. As shown in Figure 7, a clear footprint was detected with both drugs around nucleotide position 70. The site protected from cleavage by the nuclease corresponds to a GC-rich sequence. Adjoining the protected sites are a few regions where the DNAase I cutting rate is substantially enhanced relative to the control. For example, this is the case around nucleotide positions 42–47 which correspond to a row of consecutive AT base pairs. Such enhancements may

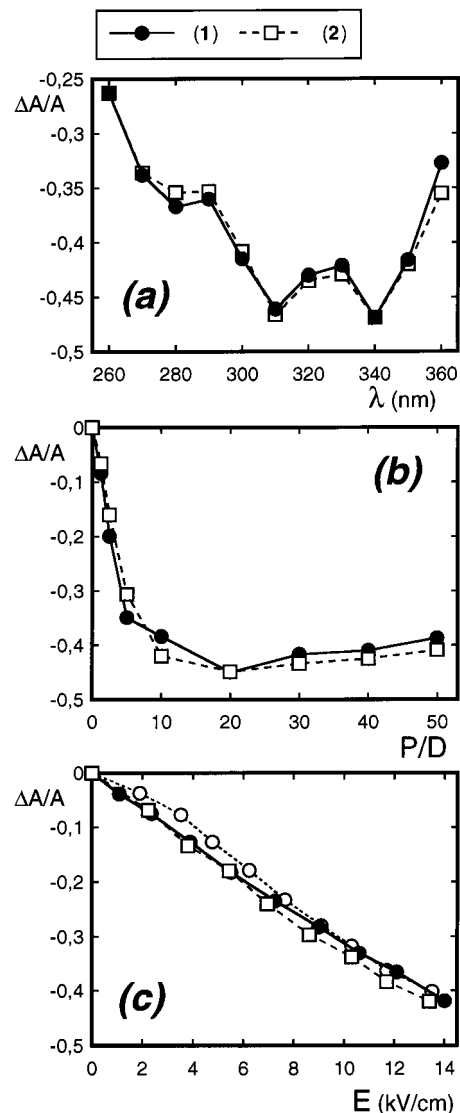


**Figure 5.** Dependence of the reduced dichroism  $\Delta A/A$  on (a) the wavelength, (b) DNA-phosphate-to-drug ratio (P/D), and (c) electric field strength. (●) **1**, (□) **2**, (○) DNA alone. Conditions: (a) P/D = 10, 12.5 kV/cm; (b) 310 nm, 12.5 kV/cm; (c) 310 nm, P/D = 20 in 1 mM sodium cacodylate buffer, pH 6.5.

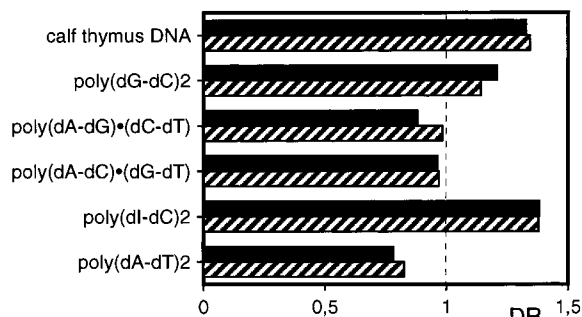


**Figure 6.** Variations of the dichroism ratio (DR) for **1** (solid bars) and **2** (hatched bars) bound to the polynucleotides of different base composition. ELD data were recorded in the presence of 200  $\mu\text{M}$  polynucleotide and 10  $\mu\text{M}$  drug, at 310 nm, in 1 mM sodium cacodylate pH 6.5, under a field strength of 13 kV/cm.

occur as a result of the local deformation of the double helix (unwinding, stiffening, and lengthening of the sugar-phosphate backbone) induced by intercalation of



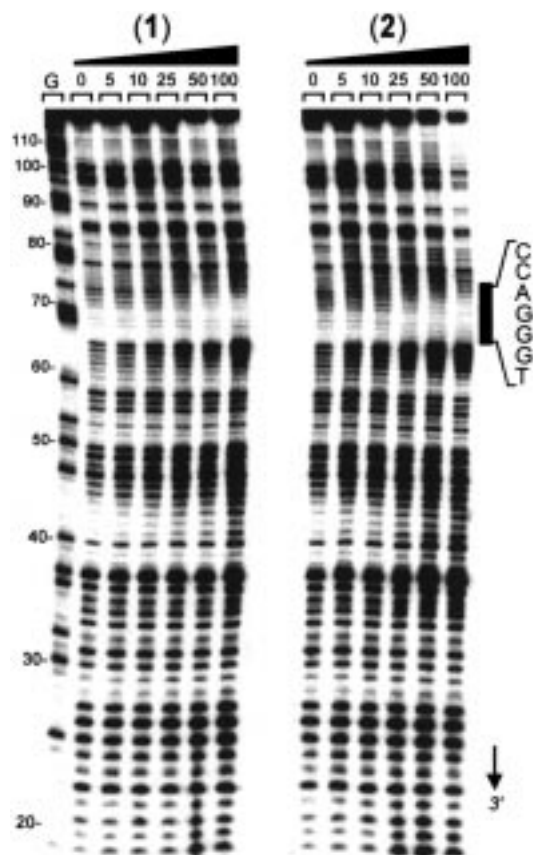


**Figure 7.** DNAase I footprinting with the 117-mer *PvuII-EcoRI* restriction fragment of plasmid pBS in the presence of the two drugs at the indicated concentration ( $\mu\text{M}$ ). The DNA was 3'-end-labeled at the *EcoRI* site with [ $\alpha$ - $^{32}\text{P}$ ]dATP in the presence of AMV reverse transcriptase. The products of nuclease digestion were resolved on an 8% polyacrylamide gel containing 7 M urea. Control tracks (0) contained no drug. Guanine-specific sequence markers obtained by treatment of the DNA with dimethyl sulfate followed by piperidine were run in the lane marked G. Numbers on the left side of the gel refer to the standard numbering scheme for the nucleotide sequence of the DNA fragment. The sequence of a preferential drug binding site is indicated.

the drug into DNA. But these regions of enhanced cleavage at sequences remote from identified sites of drug binding may also reflect the redistribution of enzyme molecules (the "mass-action" effect).<sup>28</sup> The data are consistent with other footprinting studies with rebeccamycin analogues.<sup>29</sup> Binding occurs preferentially at sequences containing GC or GT sites.

**Topoisomerase I Inhibition.** The topoisomerase I inhibitory properties of the drugs were examined using three complementary approaches. First, we resorted to a DNA relaxation assay. Negatively supercoiled plasmid pKMp27 was incubated with topoisomerase I in the presence of increasing concentration of the two drugs. The DNA samples were treated with SDS and proteinase K to remove any covalently bound protein and resolved in a 1% agarose gel containing ethidium bromide. As shown in Figure 8A, supercoiled DNA is fully relaxed by topoisomerase I in the absence of drug (compare lanes DNA and TopoI). The relaxed DNA migrates faster than the supercoiled plasmid on an agarose gel containing ethidium bromide (because of DNA unwinding effects). In the presence of the two drugs, the intensity of the band corresponding to the

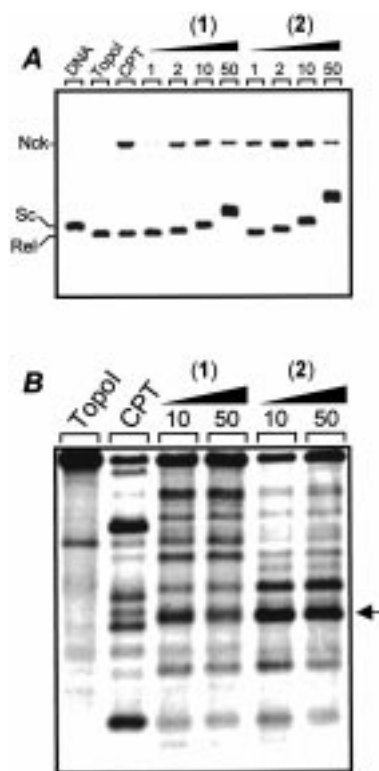


**Figure 8.** (A) Effect of increasing concentrations of **1** and **2** on the relaxation of plasmid DNA by topoisomerase I. Supercoiled DNA (lane DNA) was incubated without or with human topoisomerase I (lane TopoI) in the absence and presence of the test drug at the indicated concentration ( $\mu\text{M}$ ). DNA samples were separated by electrophoresis on an agarose gel containing ethidium bromide. The gel was photographed under UV light. Abbreviations: Nc, nicked; Rel, relaxed; Sc, supercoiled. (B) Topoisomerase I-mediated cleavage of DNA in the presence of **1** and **2**. Purified human topoisomerase I (20 units) was incubated with the *EcoRI-AvaI* restriction fragment from plasmid pKM27 (3'-end  $^{32}\text{P}$ -labeled at the *EcoRI* site) in the absence (lane TopoI) and the presence of the test ligands. Cleaved DNA fragments were analyzed on a 1% agarose gel containing 0.1% SDS in the TBE buffer. Camptothecin (lane CPT) was used at 20  $\mu\text{M}$ . The arrowhead points to the main site of topoisomerase I cleavage stimulated by **2**.

nicked form of DNA has increased significantly. This effect, observed with camptothecin, reflects the stabilization of topoisomerase I–DNA cleavable complexes. The shift in the mobility of supercoiled plasmid (form I) observed with increasing concentrations of the indolocarbazoles is attributed to a decrease in plasmid DNA linking number due to intercalation because the same effect is observed in the absence of the enzyme (data not shown). Like a rebeccamycin-type drug recently studied,<sup>30</sup> **1** and **2** can behave both as specific topoisomerase I inhibitors trapping the cleavable complexes and as nonspecific inhibitors of a DNA-processing enzyme acting via DNA binding. The stabilization of DNA–topoisomerase I covalent complexes is more pronounced with **2** than with **1**. At 1  $\mu\text{M}$ , the formation of nicked DNA species is clearly evident with **2** whereas no effect is seen with **1**. At 2  $\mu\text{M}$ , a clear effect is observed with **1** but the nicked DNA band is much more intense with **2**.

Second, we used a  $^{32}\text{P}$ -labeled linear plasmid DNA as a substrate (the *EcoRI-AvaI* restriction fragment of pKM27). The labeled DNA fragment was incubated with topoisomerase I in the presence and absence of the

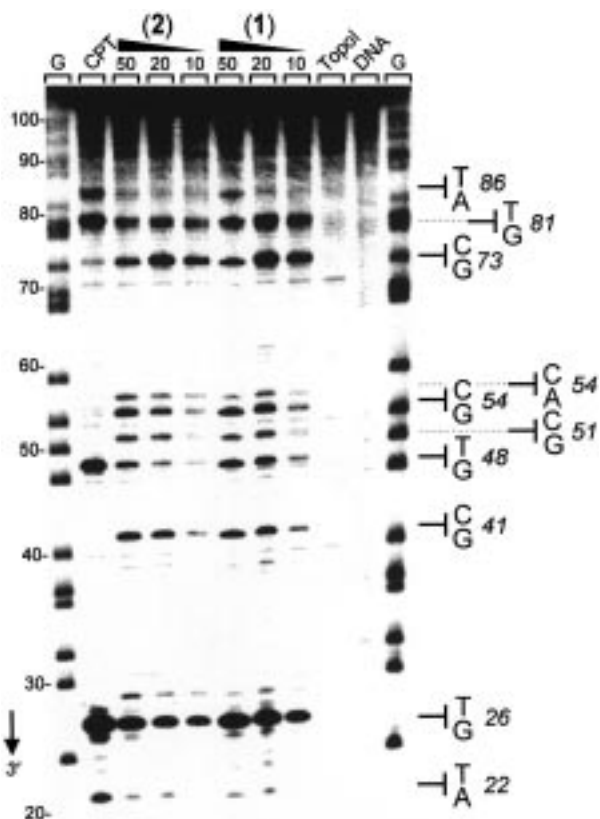


**Figure 9.** Sequencing of drug-induced topoisomerase I cleavage sites. The 117-mer DNA fragment (as used for the footprinting experiments) was subjected to cleavage by human topoisomerase I in the presence of the drugs (20–50  $\mu\text{M}$  as indicated). Cleavage products were resolved on an 8% polyacrylamide gel containing 7 M urea. Guanine-specific sequence markers obtained by treatment of the DNA with dimethyl sulfate followed by piperidine were run in the lane marked G. The control track (DNA) contained no drug and no enzyme. The lane TopoI refers to the radiolabeled DNA substrate incubated with the enzyme but with no drug. Camptothecin was used at 20  $\mu\text{M}$  (lane CPT). The positions of the main topoisomerase I cleavage sites are indicated by arrows.

indolocarbazoles, and the resulting DNA cleavage products were analyzed by agarose gel electrophoresis under alkaline conditions. The profiles of DNA cleavage, presented in Figure 8B, are different with the two drugs. One of the cleavage sites (indicated by an arrow) is much more enhanced in the presence of **2** than with **1**. Conversely, at other sites the cleavage is more intense with **1** than **2**. The chemical nature of the side chain at the N6 position seems to influence the cleavage of DNA by the enzyme. It is important to note also that the cutting profiles obtained with the two indolocarbazoles are significantly different from that obtained with camptothecin. The data in Figure 8B corroborate the hypothesis that the  $\text{NHCHO} \rightarrow \text{NHCH}(\text{CH}_2\text{OH})_2$  substitution has a significant effect on the poisoning of topoisomerase I. This observation is consistent with the model for the interaction of the drug with the enzyme–DNA complex.

Third, the 117-mer restriction fragment used for the footprinting experiments was employed to identify the sequence of the topoisomerase I cleavage sites. A typical example of a gel is shown in Figure 9. No significant difference can be seen between the two drugs. Both drugs stimulate DNA cleavage by topoisomerase I at

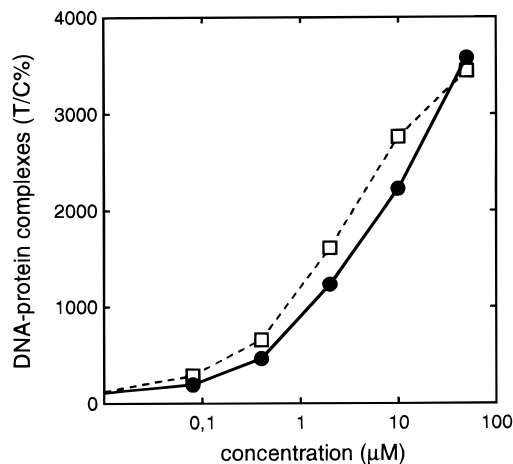


**Figure 10.** Drug-induced formation of DNA–protein complexes in HCT116 human colon cancer cells: (●) **1** and (□) **2**.

**Table 2.** Cytotoxicity [ $\text{IC}_{50}$  ( $\mu\text{M}$ )]

	<b>1</b>	<b>2</b>
P388	0.062	0.017
MKN-45	0.39	0.13
DLD-1	2.1	0.52
HCT-116	0.12	0.032

identical sites. The positions of the cleavage sites induced by the two indolocarbazoles markedly differ from those obtained with camptothecin. Compounds **1** and **2** induce DNA cleavage mainly at TG and CG sites whereas the cleavage is essentially restricted to TG steps with camptothecin. Minor cleavage sites at TA sites can occur with camptothecin (e.g., bands at positions 22 and 86) but not with the indolocarbazoles. The results agree with previous sequencing studies indicating that rebeccamycin and analogues such as NB-506 induce DNA cleavage by topoisomerase I at TG and CG sequences.<sup>22,31</sup> Apparently, there is no correspondence between the topoisomerase I cleavage sites stimulated by the drugs and the position of the preferential drug binding site on the same DNA fragment inferred from the footprinting analysis (compare Figures 7 and 9). One of the most pronounced topoisomerase I cleavage sites (at position 26) occurs some distance from the main drug binding site at the GC-rich sequence around position 70.

#### Formation of Protein–DNA Complexes in Cells.

The effect of the drugs on the formation of protein–DNA complexes in HCT116 human colon cancer cells was studied by means of a potassium/SDS precipitation assay.<sup>32</sup> Both drugs enhance the formation of the complexes in a dose-dependent manner (Figure 10). For drug concentrations from 0.4 to 10  $\mu\text{M}$  the effect is slightly more pronounced with **2** than with **1**. This is consistent with their respective DNA binding and topoisomerase I activities measured *in vitro*.

**Cytotoxicity.** Four cell lines were employed to evaluate the cytotoxicity of the drugs. The  $\text{IC}_{50}$  values are collated in Table 2. In all cases, **2** proved to be more toxic than **1**. With the murine cell line (P388), **2** is about 4 times more toxic than **1**. The difference is about the same with the two human colon cancer cells DLD-1 and HCT116. With the human gastric cancer cells MKN-45, **2** is three times more toxic than **1**. Logically, the

higher cytotoxicity of **2** compared to **1** may be attributed to the increased affinity for DNA and the enhanced poisoning activity of topoisomerase I.

## Conclusion

The above results indicate that the replacement of the NHCHO substituent of NB-506 with a longer side chain reinforces the interaction of the drug with DNA without affecting the intercalative binding process. Moreover, the new substituent seems to play a role in the interference of the drug with the DNA–topoisomerase I cleavable complexes. Indeed, the new drug is noticeably more efficient than NB-506 at inhibiting topoisomerase I. The enhanced cytotoxicity of **2** compared to **1** on four different cell lines can logically be attributed to the increased affinity of the drug for DNA and/or the superior effects on topoisomerase I. From these results, we can conclude that the introduction of a hydrophilic substituent at position 6 on the nitrogen imide represents a profitable route for the design of antitumor indolocarbazoles. It is interesting to note that the bulk and the structure of the new substituent are close to those found at the N6 position on the rebeccamycin analogue NSC#655649, which is being developed for the treatment of solid tumors, especially in children.<sup>33</sup> Novel NB-506 analogues with different types of side chains at position 6 are being synthesized.

## Experimental Section

**Drugs and Chemicals.** The two drugs were provided by Banyu Pharmaceuticals (Japan). Their chemical synthesis has been reported.<sup>34–36</sup> Camptothecin was purchased from Sigma Chemical Co. (La Verpillière, France). The drugs were first dissolved in dimethyl sulfoxide (DMSO) at 10 mM and then further diluted with water. The final DMSO concentration never exceeded 0.3% (v/v) in the cleavage reactions. Under these conditions, DMSO, which is also used in the controls, does not affect the topoisomerase activity. The stock solutions of drugs were kept at  $-20\text{ }^{\circ}\text{C}$  and freshly diluted to the desired concentration immediately prior to use (diluted solutions tend to precipitate when stored at  $4\text{ }^{\circ}\text{C}$ ). All other chemicals were analytical grade reagents.

**Biochemicals.** Restriction endonucleases *Ava*I and *Eco*RI, alkaline phosphatase, T4 polynucleotide kinase, and AMV reverse transcriptase were purchased from Boehringer (Mannheim, Germany) and used according to the supplier's recommended protocol in the activity buffer provided. Experiments were performed with either human topoisomerase I from TopoGen Inc. (Columbus, OH) or calf thymus topoisomerase I from Life Science technologies (Cergy-Pontoise, France). Calf thymus DNA and the double-stranded polymers poly(dA-dT)·poly(dA-dT), poly(dI-dC)·poly(dI-dC), poly(dA-dG)·poly(dC-dT), poly(dA-dC)·poly(dG-dT), and poly(dG-dC)·poly(dG-dC) were from Pharmacia (Uppsala, Sweden). Their concentrations were determined by applying molar extinction coefficients given in the literature.<sup>37</sup> Calf thymus DNA was deproteinized with sodium dodecyl sulfate (protein content < 0.2%), and all nucleic acids were dialyzed against 1 mM sodium cacodylate buffer pH 6.5. All solutions were prepared using doubly deionized, Millipore filtered water.

**Absorption Spectra and Melting Temperature Studies.** Melting curves were measured using an Uvikon 943 spectrophotometer coupled to a Neslab RTE111 cryostat. For each serie of measurements, 12 samples were placed in a thermostatically controlled cell holder, and the quartz cuvettes (10 mm path length) were heated by circulating water. The measurements were performed in BPE buffer pH 7.1 (6 mM  $\text{Na}_2\text{HPO}_4$ , 2 mM  $\text{NaH}_2\text{PO}_4$ , 1 mM EDTA). The temperature inside the cuvette was measured with a platinum probe; it was increased over the range 20–100  $^{\circ}\text{C}$  with a heating rate of 1  $^{\circ}\text{C}/\text{min}$ . The "melting" temperature  $T_m$  was taken as the

midpoint of the hyperchromic transition. The Uvikon 943 spectrophotometer was also used to record the absorption spectra. Titrations of the drug with DNA, covering a large range of DNA phosphate/drug ratios (P/D), were performed by adding aliquots of a concentrated DNA solution to a drug solution at constant ligand concentration (20  $\mu\text{M}$ ). DNA blanks at the same nucleotide concentrations were prepared concomitantly and used as a reference in the recording of absorption spectra.

**Fluorescence Titration Experiments.** The stock drug solutions were freshly prepared at a concentration of 5 mM in DMSO and diluted into buffer solution at the desired concentration. Calf thymus DNA was purchased from Pharmacia (lot number 27-4562-02) and was sonicated and purified as described earlier.<sup>38</sup> Before further use, the DNA was dialyzed in the appropriate buffer for 24 h, and its concentration was determined by UV absorption at 260 nm by using a molar extinction coefficient,  $\epsilon_{260} = 12\,824\text{ cm}^{-1}\text{ M}^{-1}$ . Titration experiments were carried out in a buffer (BPE) consisting of 6 mM  $\text{Na}_2\text{HPO}_4$ , 2 mM  $\text{NaH}_2\text{PO}_4$ , 1 mM  $\text{Na}_2\text{EDTA}$ , pH 7.0, unless noted otherwise. Fluorescence titration data were recorded at room temperature using I.S.S. Greg 200 fluorometer. Excitation was at 320 nm, and fluorescence emission was monitored over the range 340–620 nm. Samples used for titration experiments were prepared separately at a constant drug concentration of 5  $\mu\text{M}$  and at DNA concentrations ranging from 0.1  $\mu\text{M}$  to 1 mM bp.

Fluorescence titration data were fitted directly to get binding constants, using a fitting function incorporated into FitAll (MTR Software, Toronto). Simply, the observed fluorescence is assumed to be a sum of the weighted concentrations of free and bound ligand

$$F = F^0 (C_t - C_b) + F^b C_b \quad (1)$$

where  $F$  is the apparent fluorescence at each DNA concentration,  $F^0$  is the fluorescence intensity of free ligand, and  $F^b$  is the fluorescence intensity of the bound species. For the interaction of a ligand D with a DNA site S, it may be easily shown that

$$Kx^2 - x(KS_0 + KD_0 + 1) + KS_0D_0 = 0 \quad (2)$$

where  $x = C_b$ ,  $K$  is the association constant,  $S_0$  is the total concentration, and  $D_0$  is the total ligand concentration. Equation 2 is readily solved using the quadratic formula. Data in the form of fluorescence response  $F$  as a function of total DNA site concentration at fixed concentration of ligand may then be fit by nonlinear least-squares methods to get  $K$ ,  $F^0$ , and  $F^b$ .

**Circular Dichroism.** CD spectra were recorded on a Jobin-Yvon CD 6 dichrograph interfaced to a microcomputer. Solutions of drugs, nucleic acids, and their complexes in 1 mM sodium cacodylate buffer (pH 6.5) were scanned in 1 cm quartz cuvettes. Measurements were made by progressive dilution of drug–DNA complex at a high P/D (phosphate/drug) ratio with a pure ligand solution to yield the desired drug/DNA ratio. Three scans were accumulated and automatically averaged.

**Electric Linear Dichroism.** ELD measurements were performed using a computerized optical measurement system built by C. Houssier.<sup>39</sup> The procedures outlined previously were followed.<sup>40</sup> The optical setup incorporating a high-sensitivity T-jump instrument equipped with a Glan polarizer was used under the following conditions: bandwidth 3 nm, sensitivity limit 0.001 in  $\Delta A/A$ , response time 3  $\mu\text{s}$ . Equations used for the calculation of the different parameters have been reported.<sup>27,40</sup> All experiments were conducted at 20  $^{\circ}\text{C}$  with a 10 mm path length Kerr cell, having 1.5 mm of electrode separation, in 1 mM sodium cacodylate buffer, pH 6.5. The DNA samples were oriented under an electric field strength of 13 kV/cm, and the drug under test was present at 10  $\mu\text{M}$  together with the DNA or polynucleotide at 100  $\mu\text{M}$  unless otherwise stated. This electrooptical method has proved most useful as a means of determining the orientation of drugs bound to DNA and has the additional advantage that it senses



only the orientation of the polymer-bound ligand: free ligand is isotropic and does not contribute to the signal.<sup>41</sup>

To investigate the geometry of drug binding to DNA by ELD, the reduced dichroism  $\Delta A/A$  of a ligand-DNA complex measured in the ligand absorption band must be analyzed with respect to the reduced dichroism measured for the same DNA or polynucleotide at 260 nm in the absence of drug,  $(\Delta A/A)^{\text{DNA}}$ . The reduced dichroism ratio DR is defined as follows:  $\text{DR} = [(\Delta A/A)^{\text{ligand-DNA}}]/[(\Delta A/A)^{\text{DNA}}]$ . The numerator refers to the reduced dichroism of the drug-DNA complex measured at the absorption maximum of the ligand bound to DNA. The denominator is always negative under the experimental conditions used. The dichroism ratio is expected to be +1 if the transition moment of the drug chromophore is parallel to the DNA bases, as in the case of complete intercalative binding. For groove binders, the angle between the double helical axis and the long axis of the chromophore lies below 54° which gives rise to positive dichroism and thus to a negative DR value. Under these conditions, the reduced dichroism ratios for any given drug-DNA and drug-polynucleotide complexes can be mutually compared with good relative accuracy, independent of the polymer size.<sup>27,41</sup>

**DNA Purification and Labeling.** The plasmid pBS (Stratagene, La Jolla, CA) was isolated from *E. coli* by a standard sodium dodecyl sulfate-sodium hydroxide lysis procedure and purified using Qiagen columns. The 117-mer fragment was prepared by 3'-[<sup>32</sup>P]-end labeling of the *EcoRI*-*PvuII* double digest of the plasmid using  $\alpha$ -[<sup>32</sup>P]-dATP (Amersham, Buckinghamshire, England) and AMV reverse transcriptase. The digestion products were separated on a 6% polyacrylamide gel under native conditions in TBE buffered solution (89 mM Tris-borate pH 8.3, 1 mM EDTA). After autoradiography, the band of DNA was excised, crushed, and soaked in water overnight at 37 °C. This suspension was filtered through a Millipore 0.22  $\mu\text{m}$  filter, and the DNA was precipitated with ethanol. After the solution was washed with 70% ethanol and the precipitate was vacuum-dried, the labeled DNA was resuspended in 10 mM Tris, adjusted to pH 7.0, containing 10 mM NaCl.

**Footprinting Experiments.** Cleavage reactions by DNAase I were performed essentially according to the previously detailed protocols.<sup>42</sup> Briefly, reactions were conducted in a total volume of 10  $\mu\text{L}$ . Samples (3  $\mu\text{L}$ ) of the <sup>32</sup>P-labeled DNA fragment were incubated with 5  $\mu\text{L}$  of the buffer solution containing the desired drug concentration. After 20 min of incubation at 37 °C to ensure equilibration of the binding reaction, the digestion was initiated by the addition of 2  $\mu\text{L}$  of DNAase I (0.01 unit/mL enzyme in 20 mM NaCl, 2 mM MgCl<sub>2</sub>, 2 mM MnCl<sub>2</sub>, pH 7.3). At the end of the reaction time (routinely 4 min at room temperature), the digestion was stopped by freeze-drying. After lyophilization, each sample was resuspended in 4  $\mu\text{L}$  of an 80% formamide solution containing tracking dyes prior to electrophoresis. A Molecular Dynamics 445SI PhosphorImager was used to collect all data which were analyzed using the ImageQuant version 4.1 software. Each resolved band on the autoradiograph was assigned to a particular bond within the DNA fragment by comparison of its position relative to sequencing standards.

**DNA Relaxation Experiments.** Supercoiled pKMp27 DNA (0.5  $\mu\text{g}$ ) was incubated with 6 units of human topoisomerase I at 37 °C for 1 h in relaxation buffer (50 mM Tris pH 7.8, 50 mM KCl, 10 mM MgCl<sub>2</sub>, 1 mM dithiothreitol, 1 mM EDTA) in the presence of varying concentrations of the drug under study. Reactions were terminated by adding SDS to 0.25% and proteinase K to 250  $\mu\text{g}/\text{mL}$ . DNA samples were then added to the electrophoresis dye mixture (3  $\mu\text{L}$ ) and electrophoresed in a 1% agarose gel containing ethidium bromide (1 mg/mL), at room temperature for 4 h. Gels were washed and photographed under UV light.

**Stimulation of Topoisomerase I-Mediated DNA Cleavage.** The plasmid pKM27<sup>43</sup> was linearized with *EcoRI* and labeled with  $\alpha$ -[<sup>32</sup>P]-dATP in the presence of the Klenow fragment of DNA polymerase I. The labeled DNA was then digested to completion with *AvaI*. The cleavage reaction mixture contained 20 mM Tris HCl pH 7.4, 60 mM KCl, 0.5 mM EDTA, 0.5 mM dithiothreitol, 2  $\times$  10<sup>4</sup> dpm of  $\alpha$ -[<sup>32</sup>P]-

pKM27 DNA, and the indicated drug concentrations. The reaction was initiated by the addition of human topoisomerase I (20 units in 20  $\mu\text{L}$  reaction volume) and allowed to proceed for 10 min at 37 °C. Reactions were stopped by adding SDS to a final concentration of 0.25% and proteinase K to 250  $\mu\text{g}/\text{mL}$ , followed by incubation for 30 min at 50 °C. Samples were denatured by the addition of 10  $\mu\text{L}$  of denaturing loading buffer, consisting of 0.45 M NaOH, 30 mM EDTA, 15% (w/v) sucrose, and 0.1% bromocresol green, prior to loading on to a 1% agarose gel in TBE buffer containing 0.1% SDS. Electrophoresis was conducted at 2 V/cm for 18 h.

**Sequencing of Topoisomerase I-Mediated DNA Cleavage Sites.** Each reaction mixture contained 2  $\mu\text{L}$  of 3'-end [<sup>32</sup>P]-labeled DNA (~1  $\mu\text{M}$ ), 5  $\mu\text{L}$  of water, 2  $\mu\text{L}$  of 10X topoisomerase I buffer, and 10  $\mu\text{L}$  of drug solution at the desired concentration, usually 10–50  $\mu\text{M}$ . After at least 30 min of incubation to ensure equilibration, the reaction was initiated by addition of 20 units of calf thymus topoisomerase I. Samples were incubated for 40 min at 37 °C prior to adding SDS to 0.25% and proteinase K to 250  $\mu\text{g}/\text{mL}$  to dissociate the drug-DNA-topoisomerase I cleavable complexes. The DNA was precipitated with ethanol and then resuspended in 5  $\mu\text{L}$  of formamide-TBE loading buffer, denatured at 90 °C for 4 min, and then chilled in ice for 4 min prior to loading on to the sequencing gel.

**Tumor Cells.** HCT116 (human colon cancer) cells and DLD-1 (human colon cancer) cells were provided by Dr. N. Shindo-Okada and Dr. H. Fukazawa, respectively, of the National Cancer Center Research Institute (Tokyo, Japan). MKN-45 (human gastric cancer) cells were purchased from Immuno Biological Laboratories (Gunma, Japan). P388 (murine leukemia) cells were provided by Dr. T. Tsuruo of the Applied Microbiology, University of Tokyo. All the cells were cultured in DMEM or RPMI-1640 supplemented with 10% FBS.

**Cleavable Complex Formation in Cultured Cells.** HCT116 cells (2.5  $\times$  10<sup>5</sup>) HCT116 cells were prelabeled by the incubation with DMEM-10% FBS containing 0.5  $\mu\text{Ci}/\text{mL}$  of [<sup>3</sup>H]thymidine at 37 °C and 5% CO<sub>2</sub> overnight. The cells were washed with fresh medium and then incubated with topoisomerase I inhibitors for 1 h. Then the cells were directly lysed with a 1.5% SDS, 5 mM EDTA solution and subjected to K<sup>+</sup>/SDS precipitation assay.<sup>32</sup>

**Antitumor Spectrum in Vitro.** Cells (1  $\times$  10<sup>3</sup>) cells were plated in 96-well plates 1 day before the start of the assay. Then, diluted test compounds were added to each well, and incubation was continued for 72 h. Growth of adherent cell lines (HCT116, MKN-45, DLD-1, and colon 26) was estimated by a sulforhodamine B dye-staining method<sup>44</sup> and that of suspension cells (P388) was measured by the MTT method.<sup>45</sup>

**Acknowledgment.** C.B. thanks Brigitte Baldeyrou and Delphine Lucas for expert technical assistance. This work was done under the support of research grants (to C.B.) from the Ligue Nationale Française Contre le Cancer (Comité du Nord) and the Association pour la Recherche sur le Cancer; (to C.H. and P.C.) from the Actions de Recherches Concertées contract 95/00-193 and the FNRS, Télévie 7/4526/94; (to J.B.C.) and from the National Cancer Institute (Grant CA35635). Support by the "convention INSERM-CFB" is acknowledged.

## References

- (1) Kojiri, K.; Kondo, H.; Yoshinari, T.; Arakawa, H.; Nakajima, S.; Satoh, F.; Kawamura, K.; Okura, A.; Suda, H.; Okanishi, M. A new antitumor substance BE-13793C, produced by a streptomycete. Taxonomy, fermentation, isolation, structure determination and biological activity. *J. Antibiot.* **1991**, *44*, 723–728.
- (2) Tanaka, S.; Ohkubo, M.; Kojiri, K.; Suda, H.; Yamada, A.; Uemura, D. A new indolopyrrolo carbazole antitumor substance, ED-110, a derivative of BE-13793C. *J. Antibiot.* **1992**, *45*, 1797–1798.
- (3) Yoshinari, T.; Yamada, A.; Uemura, D.; Nomura, K.; Arakawa, H.; Kojiri, K.; Yoshida, E.; Suda, H.; Okura, A. Induction of topoisomerase I-mediated DNA cleavage by a new indolocarbazole, ED-110. *Cancer Res.* **1993**, *53*, 490–494.



- (4) Arakawa, H.; Iguchi, T.; Yoshinari, T.; Kojiri, K.; Suda, H.; Okura, A. ED-110, a novel indolocarbazole, prevents the growth of experimental tumors in mice. *Jpn. J. Cancer Res.* **1993**, *53*, 574–581.
- (5) Arakawa, H.; Iguchi, T.; Morita, M.; Yoshinari, T.; Kojiri, K.; Suda, H.; Okura, A.; Nishimura, S. Novel indolocarbazole compound 6-*N*-formylamino-12,13-dihydro-1,11-dihydroxy-13-( $\beta$ -D-glucopyranosyl)-5*H*-indolo[2,3-*a*]pyrrolo-[3,4-*c*]carbazole-5,7-(6*H*)-dione (NB-506): its potent antitumor activities in mice. *Cancer Res.* **1995**, *55*, 1316–1320.
- (6) Arakawa, H.; Matsumoto, H.; Morita, M.; Sasaki, M.; Taguchi, K.; Okura, A.; Nishimura, S. Antimetastatic effect of a novel indolocarbazole (NB-506) on IMC–HM murine tumor cells metastasized to the liver. *Jpn. J. Cancer Res.* **1996**, *56*, 518–523.
- (7) Ohe, Y.; Tanigawara, Y.; Fujii, H.; Ohtsu, T.; Wakita, H.; Igarashi, T.; Minami, H.; Eguchi, K.; Shinkai, T.; Tamura, T.; Kunotoh, H.; Saijo, N.; Okada, K.; Ogino, H.; Sasaki, Y. Phase I and pharmacology study of 5-day infusion of NB-506. *Proc. ASCO* **1997**, *16*, 199a.
- (8) Saijo, N. New chemotherapeutic agents for the treatment of nonsmall cell lung cancer. *Chest* **1998**, *113*, 17S–23S.
- (9) Yamashita, Y.; Fujii, N.; Murakata, C.; Ashizawa, T.; Okabe, M.; Nakano, H. Induction of mammalian DNA topoisomerase I mediated DNA cleavage by antitumor indolocarbazole derivatives. *Biochemistry* **1992**, *31*, 12069–12075.
- (10) Kanzawa, F.; Nishio, K.; Kubota, N.; Saijo, N. Antitumor activities of a new indolocarbazole substance, NB-506, and establishment of NB-506-resistant cell lines, SBC-3/NB. *Cancer Res.* **1995**, *55*, 2806–2813.
- (11) Vanhoef, U.; Voigt, W.; Hilger, R. A.; Yin, M.-B.; Harstrick, A.; Seeber, S.; Rustum, Y. M. Cellular determinants of resistance to indolocarbazole analogue NB-506. A novel potent topoisomerase I inhibitor, in multidrug-resistant human tumor cells. *Oncol. Res.* **1997**, *9*, 485–494.
- (12) Yoshinari, T.; Matsumoto, M.; Arakawa, H.; Okada, H.; Noguchi, K.; Suda, H.; Okura, A.; Nishimura, S. Novel antitumor indolocarbazole compound 6-*N*-formylamino-12,13-dihydro-1,11-dihydroxy-13-( $\beta$ -D-glucopyranosyl)-5*H*-indolo[2,3-*a*]pyrrolo-[3,4-*c*]carbazole-5,7-(6*H*)-dione (NB-506): induction of topoisomerase I-mediated DNA cleavage and mechanisms of cell line-selective cytotoxicity. *Cancer Res.* **1995**, *55*, 1310–1315.
- (13) Pommier, Y.; Pourquier, P.; Fan, Y.; Strumberg, D. Mechanism of action of eukaryotic DNA topoisomerase I and drugs targeted to the enzyme. *Biochim. Biophys. Acta* **1998**, *1400*, 83–106.
- (14) Pommier, Y. Diversity of DNA topoisomerases I and inhibitors. *Biochimie* **1998**, *80*, 255–270.
- (15) Bailly, C. Topoisomerase I poisons and suppressors as anticancer drugs. *Curr. Med. Chem.* **1999**, in press.
- (16) Rodrigues-Pereira E.; Belin, L.; Sancelme, M.; Prudhomme, M.; Ollier, M.; Rapp, M.; Sèverè, D.; Riou, J.-F.; Fabbro, D. Structure–activity relationships in a series of substituted indolocarbazoles: topoisomerase I and protein kinase C inhibition and antitumoral and antimicrobial properties. *J. Med. Chem.* **1996**, *39*, 4471–4477.
- (17) Anizon, F.; Belin, L.; Moreau, P.; Sancelme, M.; Voltaire, A.; Prudhomme, M.; Ollier, M.; Sèverè, D.; Riou, J.-F.; Bailly, C.; Fabbro, D.; Meyer, T. Syntheses and biological activity (topoisomerases inhibition, antitumoral and antimicrobial properties) of rebeccamycin analogues bearing modified sugar moieties and substituted on the imide nitrogen with a methyl group. *J. Med. Chem.* **1997**, *40*, 3456–3465.
- (18) Anizon, F.; Moreau, P.; Sancelme, M.; Voltaire, A.; Prudhomme, M.; Ollier, M.; Sèverè, D.; Riou, J.-F.; Bailly, C.; Fabbro, D.; Meyer, T.; Aubertin, A.-M. Syntheses, biochemical and biological evaluation of staurosporine analogues from the microbial metabolite rebeccamycin. *BioOrg. Med. Chem.* **1998**, *66*, 1597–1604.
- (19) Moreau, P.; Anizon, F.; Sancelme, M.; Prudhomme, M.; Bailly, C.; Carrasco, C.; Ollier, M.; Sèverè, D.; Riou, J.-F.; Fabbro, D.; Meyer, T.; Aubertin, A.-M. Syntheses and biological evaluation of indolocarbazoles, analogues of rebeccamycin, modified at the imide heterocycle. *J. Med. Chem.* **1998**, *41*, 1631–1640.
- (20) Moreau, P.; Anizon, F.; Sancelme, M.; Prudhomme, M.; Bailly, C.; Ollier, M.; Sèverè, D.; Riou, J.-F.; Fabbro, D.; Meyer, T.; Aubertin, A.-M. Syntheses and biological activities of rebeccamycin analogues. Introduction of a halogenoacetyl substituent. *J. Med. Chem.* **1999**, *42*, 584–592.
- (21) Bailly, C.; Qu, X.; Anizon, F.; Prudhomme, M.; Riou, J. F.; Chaires, J. B. Enhanced binding to DNA and topoisomerase I inhibition by an analogue of the antitumor antibiotic rebeccamycin containing an amino-sugar residue. *Mol. Pharmacol.* **1999**, *55*, 377–385.
- (22) Bailly, C.; Riou, J.-F.; Colson, P.; Houssier, C.; Rodrigues-Pereira, E.; Prudhomme, M. DNA cleavage by topoisomerase I in the presence of indolocarbazole derivatives of rebeccamycin. *Biochemistry* **1997**, *36*, 3917–3929.
- (23) Bailly, C.; Qu, X.; Graves, D. E.; Prudhomme, M.; Chaires, J. B. Calories from carbohydrates. Energetic contribution of the carbohydrate moiety of rebeccamycin to DNA binding and the effect of its orientation on topoisomerase I inhibition. *Chem. Biol.* **1999**, *6*, 277–286.
- (24) Friedman, R. A.; Manning, G. S. Polyelectrolyte effects on site-binding equilibria with application to the intercalation of drugs into DNA. *Biopolymers* **1984**, *23*, 2671–2714.
- (25) Record, M. T.; Anderson, C. F.; Lohman, T. M. Thermodynamic analysis of ion effects on the binding and conformational equilibria of proteins and nucleic acids: the role of ion association or release, screening, and ion effects on water activity. *Q. Rev. Biophys.* **1978**, *11*, 103–178.
- (26) Chaires, J. B. Dissecting the free energy of drug binding to DNA. *Anticancer Drug Des.* **1996**, *11*, 569–580.
- (27) Bailly, C.; Hénichart, J.-P.; Colson, P.; Houssier, C. Drug–DNA sequence-dependent interactions analysed by electric linear dichroism. *J. Mol. Recognit.* **1992**, *5*, 155–171.
- (28) Goodisman, J.; Dabrowiak, J. C. Structural changes and enhancements in DNase I footprinting experiments. *Biochemistry* **1992**, *31*, 1058–1064.
- (29) Bailly, C.; Colson, P.; Houssier, C.; Rodrigues-Pereira, E.; Prudhomme, M.; Waring, M. J. Recognition of specific sequences in DNA by a topoisomerase I inhibitor derived from the antitumor drug rebeccamycin. *Mol. Pharmacol.* **1998**, *53*, 77–87.
- (30) Labourier, E.; Riou, J. F.; Prudhomme, M.; Carrasco, C.; Bailly, C.; Tazi, J. Poisoning of topoisomerase I by an antitumor indolocarbazole drug: stabilization of topoisomerase I-DNA covalent complexes and specific inhibition of the protein kinase activity. *Cancer Res.* **1999**, *59*, 52–55.
- (31) Fukasawa, K.; Komatani, H.; Hara, Y.; Suda, H.; Okura, A.; Nishimura, S.; Yoshinari, T. Sequence-selective cleavage by a topoisomerase I poison, NB-506. *Int. J. Cancer* **1998**, *75*, 145–150.
- (32) Larsen, A. K.; Grondard, L.; Couprie, J.; Desoize, B.; Comoe, L.; Jardillier, J. C.; Riou, J. F. The antileukemic alkaloid fagaronine is an inhibitor of DNA topoisomerases I and II. *Biochem. Pharmacol.* **1993**, *46*, 1403–1412.
- (33) Weitman, S.; Moore, R.; Barrera, H.; Cheung, N. K.; Izbicka, E.; Von Hoff, D. D. In vitro antitumor activity of rebeccamycin analogue NSC655649 against pediatric solid tumors. *J. Pediatr. Hematol. Oncol.* **1998**, *20*, 136–139.
- (34) Ohkubo, M.; Kawamoto, H.; Ohno, T.; Nakano, M.; Morishima, H. Synthesis of NB-506, a new anticancer agent. *Tetrahedron* **1997**, *53*, 585–592.
- (35) Ohkubo, M.; Nishimura, T.; Jona, H.; Honma, T.; Morishima, H. Practical synthesis of indolopyrrolocarbazoles. *Tetrahedron* **1996**, *52*, 8099–8112.
- (36) Ohkubo, M.; Nishimura, T.; Jona, H.; Honma, T.; Ito, S.; Morishima, H. Synthesis of dissymmetric indolocarbazole glycosides using the Mitsunobu reaction at the glycosylation step. *Tetrahedron* **1997**, *53*, 5937–5950.
- (37) Wells, R. D.; Larson, J. E.; Grant, R. C.; Shortle, B. E.; Cantor, C. R. Physicochemical studies on polydeoxyribonucleotides containing defined repeating nucleotide sequences. *J. Mol. Biol.* **1970**, *54*, 465–497.
- (38) Chaires, J. B.; Satyanarayana, S.; Suh, D.; Fokt, I.; Przewloka, T.; Priebe, W. Parsing the free energy of anthracycline antibiotic binding to DNA. *Biochemistry* **1996**, *35*, 2047–2053.
- (39) Houssier, C.; O’Konski, C. T. Electro-optical instrumentation systems with their data acquisition and treatment. In *Molecular Electro-optics*; Krause, S., Ed.; Plenum Publishing Corporation: New York, 1981; pp 309–339.
- (40) Houssier, C. Investigating nucleic acids, nucleoproteins, polynucleotides, and their interactions with small ligands by electro-optical systems. In *Molecular Electro-optics*; Krause, S., Ed.; Plenum Publishing Corporation: New York, 1981; pp 363–398.
- (41) Colson, P.; Bailly, C.; Houssier, C. Electric linear dichroism as a new tool to study sequence preference in drug binding to DNA. *Biophys. Chem.* **1996**, *58*, 125–140.
- (42) Bailly, C.; Waring, M. J. Comparison of different footprinting methodologies for detecting binding sites for a small ligand on DNA. *J. Biomol. Struct. Dyn.* **1995**, *12*, 869–898.
- (43) Drew, H. R.; Weeks, J. R.; Travers, A. A. Negative supercoiling induces spontaneous unwinding of bacterial promoter. *EMBO J.* **1985**, *4*, 1025–1032.
- (44) Skehan, P.; Storeng, R.; Scudiero, D.; Monks, A.; MaMahon, J.; Vistica, D.; Warren, J. T.; Bokesch, S.; Boyd, M. R. New colorimetric cytotoxicity assay for anticancer-drug screening. *J. Natl. Cancer Inst.* **1990**, *82*, 1107–1112.
- (45) Rubinstein, L. V.; Shoemaker, R. H.; Paull, K. D.; Simon, R. M.; Tosini, S.; Skehan, P.; Scudiero, D. A.; Monks, A.; Boyd, M. R. Comparison of in vitro anticancer-drug-screening data generated with a tetrazolium assay versus a protein assay against diverse panel of human tumor cell lines. *J. Natl. Cancer Inst.* **1990**, *82*, 1113–1118.